(Received 18 September 2025, Accepted 15 November 2025, Scheduled 5 December 2025)

Curved Parasitic Element-Based Quad-Element Antenna for High-Gain Millimeter Wave 5G Communications

Manish K. Dabhade* and Krishna K. Warhade

Department of Electrical and Electronics Engineering, Dr. Vishwanath Karad MIT World Peace University, Pune, India

ABSTRACT: This paper proposes a novel four-port MIMO antenna specifically designed for millimeter-wave (mm-wave) 5G applications. The antenna features a compact symmetric layout measuring 22 mm × 22 mm, corresponding to approximately $2.7\lambda \times 2.7\lambda$ at 37 GHz. The prototype is fabricated on a Rogers RT Duroid 5880 substrate ($\varepsilon_r = 2.2$, $\tan\delta = 0.0009$, $h = 0.8$ mm) to ensure low loss and stable performance at high frequencies. The antenna operates effectively over two targeted frequency bands, 37–41 GHz and 42–43.5 GHz, making it suitable for high-data-rate, short-range communication systems in emerging 5G networks. The structure is evolved through multiple design stages using strategically placed curved parasitic elements to achieve dual-band operation, high isolation, and enhanced gain. Experimental validation using a vector network analyzer and anechoic chamber confirms good agreement between simulated and measured S-parameters, with isolation better than −20 dB. The antenna demonstrates a measured gain between 9.3 and 9.7 dBi, with simulated peaks up to 11 dBi. Far-field pattern measurements exhibit stable bidirectional radiation with low cross-polarization and well-defined main lobes at both 38 GHz and 42 GHz. MIMO performance metrics such as ECC < 0.01, DG ≈ 10 dB, MEG ≈ -3 dB, and CCL < 0.4 bps/Hz confirm efficient multi-port operation. The proposed antenna thus offers a compact, high-isolation, high-gain solution for next-generation mm-wave 5G MIMO systems.

1. INTRODUCTION

The demand for high-performance millimeter-wave (mm-wave) MIMO antennas in 5G systems has led to substantial research in compact, multi-port, and high-isolation antenna designs. Early studies explored planar dual-band MIMO antennas targeting the 27/39 GHz bands, demonstrating feasible size and reasonable isolation, making them suitable for initial 5G deployments [1]. To further address the mutual coupling issue inherent in compact arrays, researchers integrated defected ground structures (DGSs) and electromagnetic bandgap (EBG) techniques to achieve improved port isolation and reduced envelope correlation coefficients (ECCs) [2, 3]. For instance, coplanar waveguide (CPW)-fed and metamaterial-based multiple-input multiple-output (MIMO) configurations have gained popularity due to their compactness, wide bandwidth, and favourable radiation properties [4, 5]. Several designs targeted 28 and 38 GHz dual-band operation with novel configurations such as inverted-L-shaped, slot-loaded, and dielectric resonator antenna (DRA)-inspired antennas, offering omnidirectional coverage and wideband operation while maintaining low-profile geometries [6–8]. The use of metasurfaces, resonators, and mutual coupling suppression techniques has shown significant promise, particularly in multi-element arrays that aim for pattern diversity and polarization agility [9, 10]. Circular polarization has also been investigated to enhance link reliability, especially in mobile environments prone to multipath fading [11, 12].

High port count designs (4-port and above) with enhanced diversity performance were proposed using connected ground structures and isolation enhancement features like cross-shaped or star-slot elements [13–15]. Research has also focused on frequency-selective decoupling mechanisms and spatial diversity, enabling efficient MIMO performance across broader frequency ranges, including 27–29 GHz, 33–35 GHz, and beyond [16, 17]. Moreover, novel antenna geometries are inspired by nature and employ techniques like beam tilting, metamaterials, inverted-F arrays further refined gain, isolation, and reconfigurability for future 5G use cases [18–20]. Advanced designs have incorporated self-isolation features and multiband capabilities, addressing both uplink and downlink requirements of emerging 5G standards [21–23]. Recent contributions emphasize the role of hybrid dielectric and substrate-integrated waveguide structures in improving antenna gain and front-to-back ratios without increasing form factor [24, 25]. In addition, practical designs using cost-effective FR4 or Rogers substrates with defect-engineered ground planes have enabled scalable manufacturing potential for commercial 5G networks [26–28]. In summary, the literature reveals a clear progression toward compact, wideband, circularly polarized, and low-ECC MIMO antennas, optimized for high data rates, low latency, and robust signal integrity in complex 5G propagation environments [29].

Despite significant advancements in mm-wave MIMO antenna systems for 5G applications, several limitations persist in existing designs. Many reported antennas primarily focus on dual-band operation (e.g., 28/38 GHz) [1, 6, 18], with limited exploration into compact multi-port configurations that simultaneously achieve high isolation, circular polarization, and

* Corresponding author: Manish Kumar Dabhade (manishdabhade2114@gmail.com).

TABLE 1. Various design parameters of the proposed antenna.

Parameters	L	W	$L1$	$W1$	R	$R1$	$R2$	$R3$	$R4$	$R5$	$R6$	$R7$
Values (mm)	22	22	10.7	1.06	4.5	4.1	3.3	2.6	0.6	0.5	0.4	0.3

wide bandwidth. Moreover, techniques like EBG, DGS, and metasurfaces have improved isolation and coupling [2, 3, 5, 9] but often at the cost of increased design complexity, limited scalability, or reduced fabrication practicality, especially when using low-cost substrates like FR4. Additionally, while some studies incorporate circular polarization [4, 11, 12], they typically do not address multi-port operation with consistent axial ratio performance across all ports. Furthermore, several antennas are large in size relative to the wavelength [7, 20, 27], limiting their integration in modern compact 5G devices.

The proposed four-port MIMO antenna effectively addresses several key research gaps identified in the literature on millimeter-wave (mm-wave) 5G antenna systems. While many existing designs focus on dual-port or dual-band configurations with moderate gain and limited isolation [1–29], the proposed antenna features a compact symmetric layout measuring just 22 mm $\times$ 22 mm (approximately $2.7\lambda \times 2.7\lambda$ at 37 GHz), making it well suited for integration into space-constrained 5G devices. It operates across two distinct mm-wave bands — 37–41 GHz and 42–43.5 GHz — extending beyond the conventional 28/38 GHz bands targeted in previous studies [5, 17]. By incorporating strategically placed curved parasitic elements, the antenna achieves high inter-element isolation better than -20 dB and maintains low envelope correlation coefficient (ECC < 0.01), both of which are critical for effective MIMO operation and are often not achieved simultaneously in prior works [3, 9, 20]. The design also demonstrates enhanced gain performance, with measured gains between 9.3 and 9.7 dBi and simulated gains up to 11 dBi, surpassing many previously reported compact designs [4, 10, 13]. Additionally, stable bidirectional radiation patterns with low cross-polarization, along with favourable MIMO metrics, such as diversity gain ($<$ 10 dB), mean effective gain ($<$ -3 dB), and channel capacity loss (< 0.4 bps/Hz), confirm the antenna's suitability for robust, high-performance 5G mm-wave applications. Thus, the proposed antenna successfully fills the gap by delivering a compact, dual-band, high-isolation MIMO solution validated through both simulation and measurement.

2. ANTENNA DESIGN AND ANALYSIS

Figure 1 illustrates the geometry and dimensional details of the proposed four-element millimeter-wave MIMO antenna array, while Table 1 lists the corresponding optimized design parameters. The antenna is printed on a 0.8 mm thick RT Duroid 5880 substrate ($\varepsilon_r = 2.2$, $\tan\delta = 0.0009$), chosen for its low dielectric loss and excellent stability at mm-wave frequencies. The design incorporates four identical radiating elements (Ant 1–Ant 4) arranged orthogonally at the four corners of the substrate to achieve spatial and polarization diversity, thereby enhancing isolation and MIMO performance. Each element features a

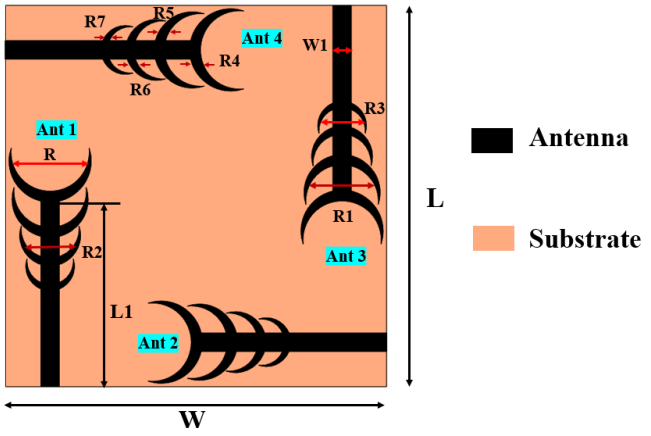

FIGURE 1. Structure and detailed dimensions of proposed four-element mm-wave antenna.

multi-resonant crescent-shaped radiator with progressively decreasing radii (R–R7), as specified in Table 1, which aids in achieving wideband impedance matching and efficient radiation characteristics. The feed line width ($W1 = 1.06$ mm) is optimized for 50 Ω impedance matching. With an overall compact size of 22 $\times$ 22 mm^2, the proposed antenna is well suited for integration in 5G and millimeter-wave wireless systems requiring compactness, high gain, and low mutual coupling.

Figure 2(a) illustrates the simulated reflection coefficients (S_{11}, S_{22}, S_{33}, S_{44}) of the proposed four-port MIMO antenna. The shaded frequency regions from 37–41 GHz and 42–43.5 GHz indicate the operational bands where all four ports exhibit reflection coefficients below the -10 dB threshold. This confirms good impedance matching and minimal return loss within these ranges, ensuring effective power transfer and resonance performance for each element — suitable for targeted millimeter-wave 5G applications. Figure 2(b) shows the corresponding transmission coefficients (S_{ij}, where $i \neq j$), representing the isolation between ports. The transmission coefficient values across the frequency range of 36–44.5 GHz remain less than -15 dB within the highlighted bands, indicating excellent isolation between antenna elements. This low mutual coupling supports enhanced MIMO functionality by minimizing channel correlation and optimizing spatial diversity. Overall, Figure 2(a) and Figure 2(b) demonstrate that the antenna performs efficiently over the specified frequency bands, meeting the requirements for high-frequency multi-port communication systems.

The radiation mechanism of the proposed antenna is governed by the coupling between the semi-circular radiating patch and the surrounding curved parasitic elements. In Step 1, (Figure 3(a)) only the fundamental TM_{11} mode of the patch is excited, producing a single resonance. With the introduction

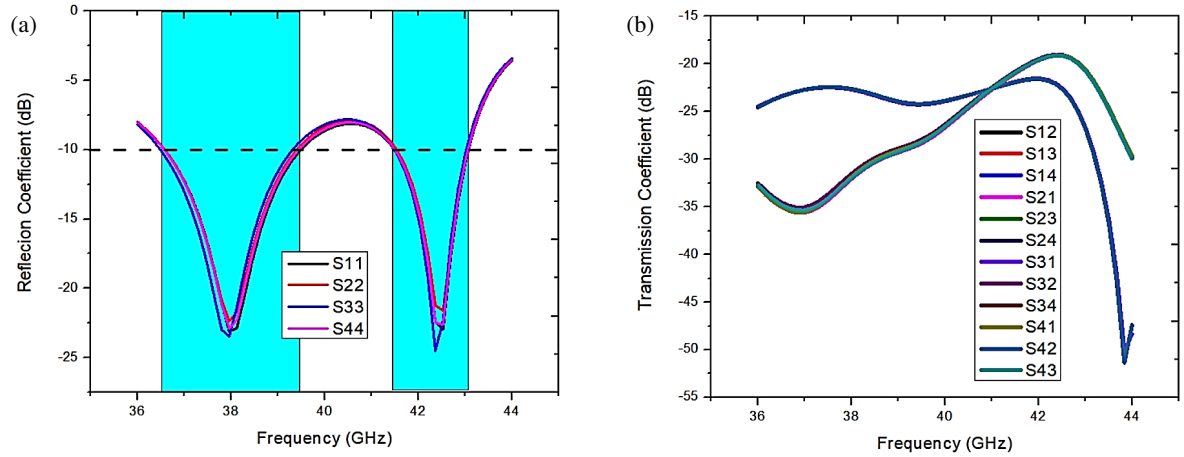

FIGURE 2. Simulated S parameters. (a) Reflection coefficient, (b) transmission coefficient.

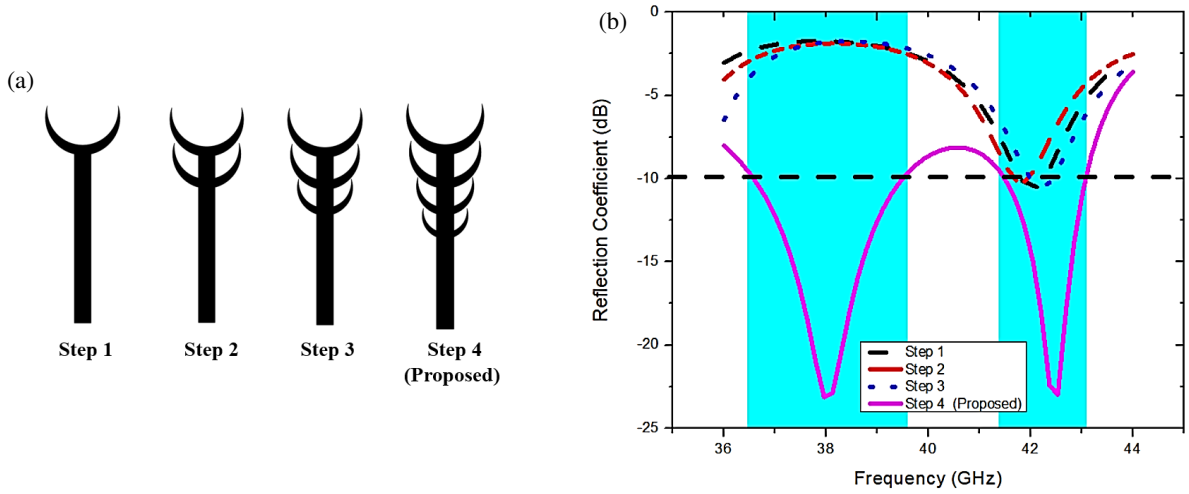

FIGURE 3. (a) Evolving stages of the proposed antenna, (b) corresponding reflection coefficient.

of successive parasitic arcs (Steps 2–3), capacitive and inductive coupling paths are established, altering the surface current distribution and generating additional resonant modes. In Step 4, the outermost curved arc introduces an additional current loop with a longer electrical path length, resulting in a lower-frequency resonance near 38 GHz, while the inner arcs sustain a higher-frequency mode near 42 GHz. The combined structure thus achieves a dual-resonant response through hybrid coupling of multiple current paths, confirming the dual-band operation observed in Figure 3(b). Figure 4 illustrates the fabricated prototype of the proposed antenna.

Figure 5 presents the measured S-parameters of the fabricated four-port MIMO antenna to experimentally validate its performance. The measurements were conducted using a vector network analyzer (VNA) in a controlled environment, with each port terminated in a 50-ohm load during individual measurements to ensure accurate S-parameter extraction. Figure 5(a) shows the measured reflection coefficients (S_{11}, S_{22}, S_{33}, S_{44}) over the 36–44.5 GHz frequency range. The highlighted bands from 37–41 GHz and 42–43.5 GHz represent the intended operating ranges. Within these regions, all four ports exhibit reflection coefficients below the -10 dB threshold, indicating good impedance matching and minimal return loss. This confirms that the antenna resonates efficiently and supports effective power transfer during real-world operation. Figure 5(b) depicts the measured transmission coefficients (S_{ij}, $i \neq j$), which reflect the mutual coupling between different antenna elements. The low coupling minimizes signal interference and correlation, making the antenna appropriate for multiport MIMO systems. Overall, the measured results in Figure 5(a) and Figure 5(b) show strong agreement with the simulated performance, validating the design's effectiveness and its applicability for millimeter-wave 5G MIMO applications.

Figure 6 presents the simulated and measured far-field radiation patterns of the proposed antenna at two key operating frequencies: 38 GHz in Figure 6(a) and 42 GHz in Figure 6(b). The measurements were carried out in an anechoic chamber using a standard far-field setup. The antenna under test (AUT) was placed on a rotating platform, and a calibrated receiving antenna measured the radiated fields as the AUT was rotated through 360° in the azimuthal plane. Both subfigures illustrate the E-plane ($\phi = 0°$) and H-plane ($\theta = 90°$) compo-

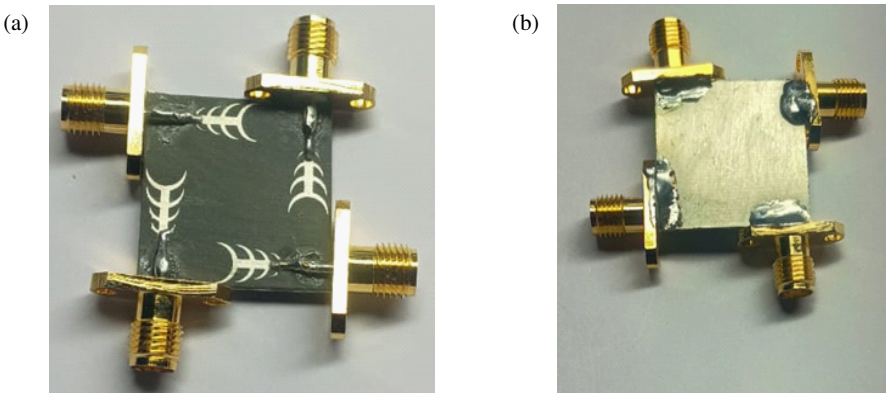

FIGURE 4. Fabricated prototype of the proposed antenna.

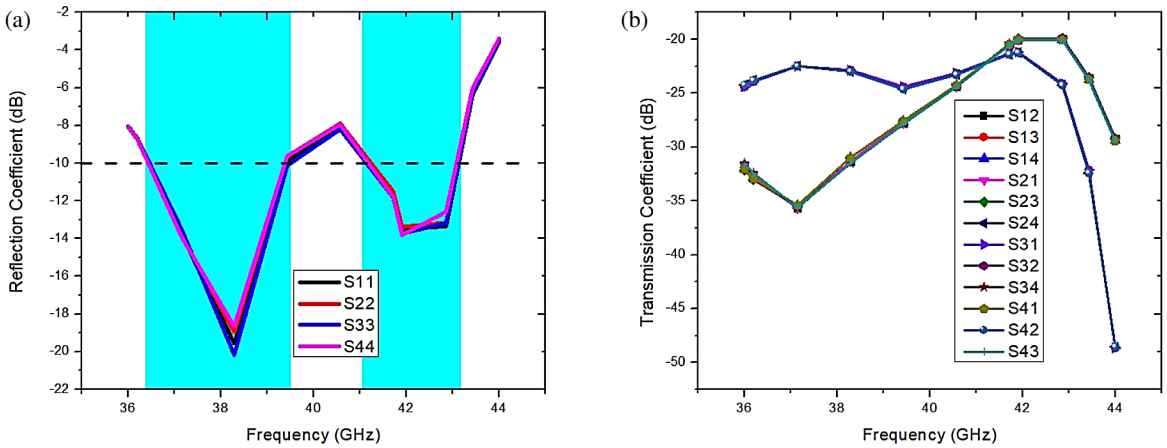

FIGURE 5. Measured S parameters. (a) Reflection coefficient, (b) transmission coefficient.

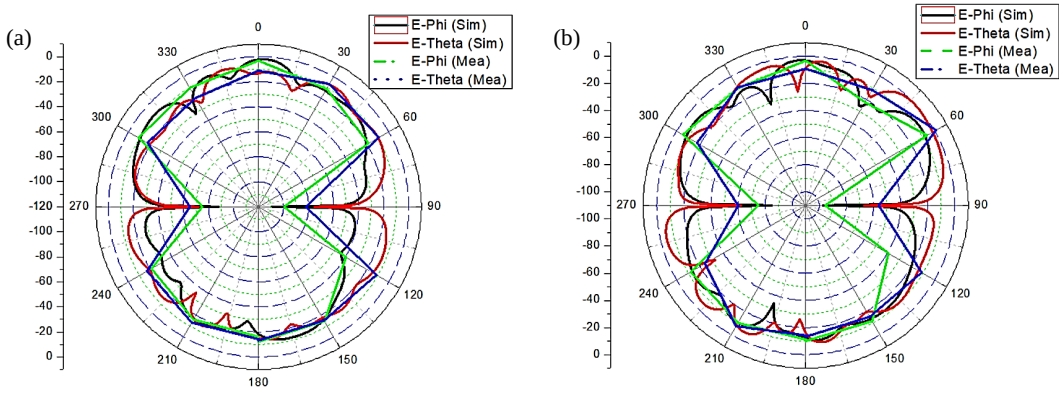

FIGURE 6. Simulated and measured normalized gain patterns of the proposed antenna at (a) 38 GHz, (b) 42 GHz.

nents of the radiation pattern. The comparison between simulated and measured results shows good agreement at both frequencies. The antenna exhibits a bidirectional radiation pattern with well-formed main lobes and relatively low cross-polarization, indicating good polarization performance. **The outermost curved parasitic element slightly extends the effective aperture, resulting in a smoother main lobe and stable bidirectional radiation behaviour without introducing asymmetry or gain distortion. The cross-polarization level remains below −20 dB within the main beam at both 38 GHz and 42 GHz, confirming excellent polarization purity.**

The radiation pattern illustrates both co- and cross-polarized components for the antenna in terms of E-theta and E-phi fields. The dominant co-polarized component maintains a maximum around 0 dB, whereas the cross-polarized component remains approximately 20 to 25 dB lower across the main lobe region. It indicates that the antenna exhibits excellent polarization pu-

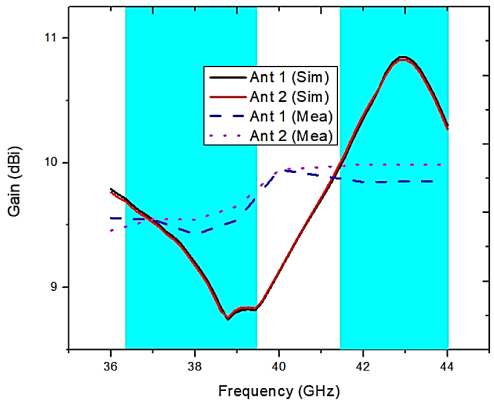

FIGURE 7. Simulated and measured gains of the proposed antenna.

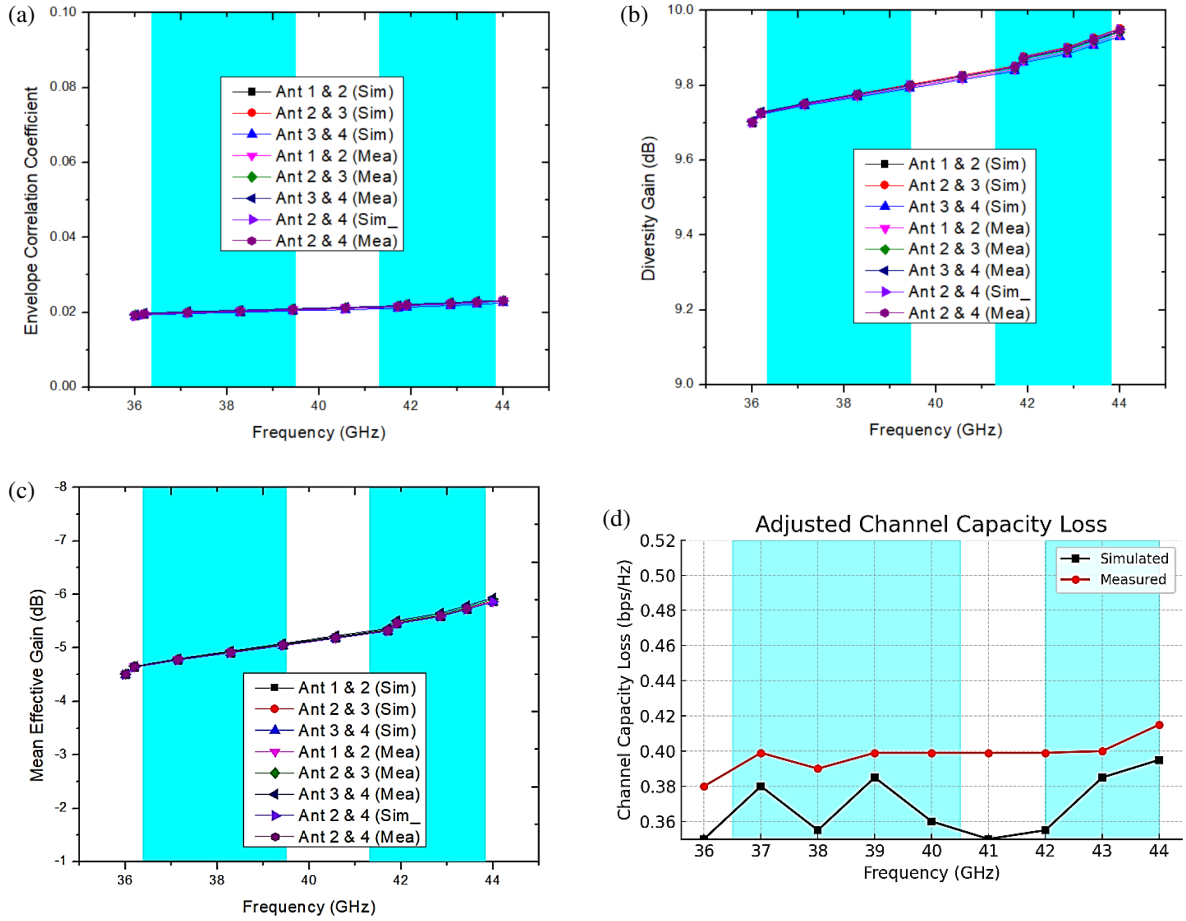

FIGURE 8. Simulated and measured MIMO parameters, (a) ECC, (b) diversity gain, (c) mean effective gain, (d) channel capacity loss.

rity with a cross-polarization level about −20 to −25 dB. Minor deviations between the simulated and measured patterns — such as slight distortions or asymmetries — can be attributed to fabrication tolerances, material imperfections, or measurement setup influences. Overall, the results confirm that the proposed antenna maintains stable and predictable radiation behaviour across its operating frequencies, reinforcing its suitability for millimeter-wave MIMO applications.

Figure 7 presents the simulated and measured gains of the proposed antenna for two ports (Antenna 1 and Antenna 2) across the frequency range of 36 to 45 GHz. The measurements were performed using a gain comparison method in an anechoic chamber, where the antenna under test (AUT) was compared against a standard gain horn antenna under identical conditions. The shaded regions from 37–41 GHz and 42–43.5 GHz mark the targeted operational bands. The simulated gain for both antenna ports shows a rising trend within the operating bands,

TABLE 2. Comparison of proposed design with state-of-the-art antenna systems.

Ref.	Antenna Size (mm^3)	Operating Frequency (GHz)	Gain (dBi)	Dielectric material	Permittivity	Mutual Coupling (dB)	ECC	CCL (bps/Hz)
[1]	26×11	26–29; 36–41	5	Ro 4003C	3.55	-30.25	0.0001	NG
[2]	$30 \times 35 \times 0.76$	25.5–29.6	8.3	Rogers	3.66	-17	0.01	0.4
[10]	$27.65 \times 12 \times 0.273$	26–30; 36.4–41.5	5.2; 5.3	RO4003	3.55	-20	0.00005	0.4
[13]	$48 \times 12 \times 0.254$	24–34; 37.5–41.5	5.7	RO5880	2.3	-20	0.00015	NG
[23]	$30 \times 15 \times 0.203$	25.5–30; 35–40	5.7	RO4003	3.55	-32.3	0.0001	NG
[29]	$26 \times 14 \times 0.38$	26.65–29.2; 36.95–39.05	1.27; 1.83	Duroid 5880	2.2	-20	0.001	0.4
[30]	$31 \times 42 \times 0.4$	Multi-band (mm-wave)	varies (reported)	Rogers RT Duroid 5880 ($\varepsilon_r = 2.2$)	2.2	-20	0.001	NG
[31]	$31 \times 42 \times 0.4$	Tri-band (NR-FR2 bands)	reported	Rogers RT Duroid 5880 ($\varepsilon_r = 2.2$)	2.2	-20	0.001	NG
[32]	Not stated	28/37 GHz (example)	~ 8 dBi (reported)	RO4003/ Rogers	3.55	-21	≈ 0.005	NG
Proposed	$22 \times 22 \times 0.8$	37–41 GHz and 42–43.5 GHz	9.3–9.7 dBi	Rogers RT Duroid 5880	2.2	-20	0.01	0.33–0.4

peaking at approximately 11 dBi near 43 GHz. The measured gain values remain fairly stable between 9.3 and 9.7 dBi, confirming acceptable performance and validating the simulation results, though with a slightly flatter profile due to practical losses such as dielectric loss, fabrication tolerances, and connector imperfections. Overall, Figure 7 demonstrates that the proposed antenna provides consistent and high gain over the intended frequency ranges, making it a strong candidate for high-frequency, high-capacity mm-wave MIMO applications.

Figure 8 illustrates the MIMO performance parameters of the proposed four-port antenna across the frequency range of 36–45 GHz, emphasizing the operational bands of 37–41 GHz and 42–43.5 GHz.

Envelope Correlation Coefficient (ECC), shown in Figure 8(a), quantifies the correlation between any two antenna elements and is calculated from the S-parameters using

$$\rho_{ij} = \frac{|S_{ii}^* S_{ij} + S_{ji}^* S_{jj}|^2}{(1 - |S_{ii}|^2 - |S_{ji}|^2)(1 - |S_{jj}|^2 - |S_{ij}|^2)}.$$

ECC values below 0.01 indicate excellent isolation and low signal correlation among the elements.

he **Diversity Gain (DG)**, defined as

$$DG = 10\sqrt{1 - |\rho_{ij}|^2}\,\text{dB},$$

is plotted in Figure 8(b) and remains close to the ideal 10 dB, confirming strong diversity performance.

Mean Effective Gain (MEG), representing the average received power of each port, is given by

$$MEG_i = \frac{1}{2}\left(1 - \sum_{j \neq i} |S_{ij}|^2\right),$$

and remains near -3 dB for all antenna pairs, as shown in Figure 8(c).

Finally, Figure 8(d) presents the **Channel Capacity Loss (CCL)**, determined from

$$CCL = -\log_2 \det(\Psi^R), \quad \Psi^R = (1 - |S|^2),$$

where smaller values correspond to minimal degradation in system capacity. Both simulated and measured CCL values are below 0.4 bps/Hz, demonstrating the antenna's suitability for efficient multi-port MIMO operation. Overall, these results validate that the proposed antenna offers robust MIMO performance with low ECC, high DG, well-balanced MEG, and minimal CCL, making it highly suitable for advanced millimeter-wave 5G applications.

As listed in Table 2, the proposed antenna exhibits substantial performance in terms of several parameters compared with reported literature. Despite its compact footprint of $22 \times 22 \times$

$0.8\,\text{mm}^3$, it achieves a higher gain of 9.3–9.7 dBi, outperforming all other referenced antennas, most of which offer gains between 1.27 and 8.4 dBi. Its dual-band operation in the 37–41 GHz and 42–43.5 GHz ranges targets upper mm-wave 5G applications, which are not simultaneously covered by many earlier designs. While some antennas like [21] support higher frequencies, they do so with significantly lower gains and larger board sizes. Moreover, the proposed antenna maintains a competitive isolation level of -20 dB, which meets the MIMO performance standard, while some designs such as [26] fall short at -17 dB. In terms of ECC, the proposed design maintains a low value of 0.01, ensuring minimal inter-element correlation and robust MIMO capability, comparable to or better than many existing works. Additionally, the channel capacity loss (CCL) is kept to 0.33 bps/Hz, which is within the acceptable range and slightly better than many referenced designs that report values up to 0.4 bps/Hz. Overall, the proposed antenna achieves a well-balanced trade-off among compact size, high gain, wide dual-band operation, and excellent MIMO performance, making it more effective and application-ready for next-generation 5G mm-wave systems.

3. CONCLUSION

A compact four-element MIMO antenna has been successfully designed, fabricated, and validated for mm-wave 5G communication, with overall dimensions of 22 mm $\times$ 22 mm, corresponding to $2.7\lambda \times 2.7\lambda$ at 37 GHz. The proposed antenna operates efficiently in the 37–41 GHz and 42–43.5 GHz bands, fulfilling the bandwidth and performance requirements of 5G millimeter-wave systems. The fabricated prototype, tested using standard measurement setups, confirms good agreement with simulation, both in terms of reflection and transmission coefficients. The antenna achieves a stable gain in the range of 9.3–9.7 dBi, with directional far-field patterns and low cross-polarization at critical frequencies. Moreover, the MIMO metrics — low ECC, high DG, near-ideal MEG, and low CCL — further validate the antenna's capability for reliable multi-port operation with minimal performance degradation. Overall, the design demonstrates a balanced combination of compact size, high gain, and excellent isolation, confirming its potential for the use in advanced high-frequency MIMO systems for 5G applications.

REFERENCES

[1] Ali, W., S. Das, H. Medkour, and S. Lakrit, "Planar dual-band 27/39 GHz millimeter-wave MIMO antenna for 5G applications," *Microsystem Technologies*, Vol. 27, No. 1, 283–292, 2021.

[2] Khalid, M., S. I. Naqvi, N. Hussain, M. Rahman, Fawad, S. S. Mirjavadi, M. J. Khan, and Y. Amin, "4-Port MIMO antenna with defected ground structure for 5G millimeter wave applications," *Electronics*, Vol. 9, No. 1, 71, 2020.

[3] Aggarwal, R., A. Roy, and R. Kumar, "Millimeter wave antennas: A state-of-the-art survey of recent developments, principles, and applications," *Progress In Electromagnetics Research B*, Vol. 104, 147–169, 2024.

[4] Patel, A., A. Desai, I. Elfergani, A. Vala, H. Mewada, K. Mahant, S. Patel, C. Zebiri, J. Rodriguez, and E. Ali, "UWB CPW fed 4-port connected ground MIMO antenna for sub-millimeter-wave 5G applications," *Alexandria Engineering Journal*, Vol. 61, No. 9, 6645–6658, 2022.

[5] Rahman, S., X.-C. Ren, A. Altaf, M. Irfan, M. Abdullah, F. Muhammad, M. R. Anjum, S. N. F. Mursal, and F. S. AlKahtani, "Nature inspired MIMO antenna system for future mmWave technologies," *Micromachines*, Vol. 11, No. 12, 1083, 2020.

[6] Megahed, A. A., E. H. Abdelhay, M. Abdelazim, and H. Y. M. Soliman, "5G millimeter wave wideband MIMO antenna arrays with high isolation," *EURASIP Journal on Wireless Communications and Networking*, Vol. 2023, No. 1, 61, 2023.

[7] Singh, S. V., J. Pratap, A. Singh, S. Sharma, and S. Gupta, "Isolation enhancement of MIMO antenna for millimeter wave applications," in *2021 2nd International Conference on Intelligent Engineering and Management (ICIEM)*, 466–470, London, United Kingdom, 2021.

[8] Shariff, P., P. R. Mane, P. Kumar, T. Ali, and M. G. N. Alsath, "Planar MIMO antenna for mmWave applications: Evolution, present status & future scope," *Heliyon*, Vol. 9, No. 2, e13362, 2023.

[9] Jayanthi, K. and A. M. Kalpana, "Design of six element MIMO antenna with enhanced gain for 28/38 GHz mm-Wave 5G wireless application," *Computer Systems Science and Engineering*, Vol. 46, No. 2, 1689–1705, 2023.

[10] Sabek, A. R., W. A. E. Ali, and A. A. Ibrahim, "Minimally coupled two-element MIMO antenna with dual band (28/38 GHz) for 5G wireless communications," *Journal of Infrared, Millimeter, and Terahertz Waves*, Vol. 43, No. 3, 335–348, 2022.

[11] Patel, A., A. Vala, A. Desai, I. Elfergani, H. Mewada, K. Mahant, C. Zebiri, D. Chauhan, and J. Rodriguez, "Inverted-L shaped wideband MIMO antenna for millimeter-wave 5G applications," *Electronics*, Vol. 11, No. 9, 1387, 2022.

[12] Iqbal, A., A. Basir, A. Smida, N. K. Mallat, I. Elfergani, J. Rodriguez, and S. Kim, "Electromagnetic bandgap backed millimeter-wave MIMO antenna for wearable applications," *IEEE Access*, Vol. 7, 111 135–111 144, 2019.

[13] Munir, M. E., S. H. Kiani, H. S. Savci, M. Marey, J. Khan, H. Mostafa, and N. O. Parchin, "A four element mm-Wave MIMO antenna system with wide-band and high isolation characteristics for 5G applications," *Micromachines*, Vol. 14, No. 4, 776, 2023.

[14] Esmail, B. A. F. and S. Koziel, "Design and optimization of metamaterial-based highly-isolated MIMO antenna with high gain and beam tilting ability for 5G millimeter wave applications," *Scientific Reports*, Vol. 14, No. 1, 3203, 2024.

[15] Elalaouy, G. M. E., Ouafae and and J. Foshi, "Mutual coupling reduction of a two-port MIMO antenna using defected ground structure," *e-Prime — Advances in Electrical Engineering, Electronics and Energy*, Vol. 8, 100557, 2024.

[16] Abbas, M. A., A. Allam, A. Gaafar, H. M. Elhennawy, and M. F. A. Sree, "Compact UWB MIMO antenna for 5G millimeter-wave applications," *Sensors*, Vol. 23, No. 5, 2702, 2023.

[17] Alfakhri, A., "Dual polarization and mutual coupling improvement of UWB MIMO antenna with cross shape decoupling structure," *e-Prime — Advances in Electrical Engineering, Electronics and Energy*, Vol. 4, 100130, 2023.

[18] Murthy, N., "Improved isolation metamaterial inspired mm-Wave MIMO dielectric resonator antenna for 5G application," *Progress In Electromagnetics Research C*, Vol. 100, 247–261, 2020.

[19] Kumar, A., A. Kumar, P. J. Soh, and A. Kumar, "Design consideration, challenges and measurement aspects of 5G mm-Wave antennas: A review," *Progress In Electromagnetics Research B*, Vol. 96, 39–66, 2022.

[20] Tariq, S., S. I. Naqvi, N. Hussain, and Y. Amin, "A metasurface-based MIMO antenna for 5G millimeter-wave applications," *IEEE Access*, Vol. 9, 51 805–51 817, 2021.

[21] Hussain, N. and N. Kim, "Integrated microwave and mm-Wave MIMO antenna module with 360° pattern diversity for 5G internet of things," *IEEE Internet of Things Journal*, Vol. 9, No. 24, 24 777–24 789, 2022.

[22] Abo-Elhassan, M. A., A. E. Farahat, and K. F. A. Hussein, "Millimetric-wave quad-band MIMO antennas for future generations of mobile communications," *Progress In Electromagnetics Research B*, Vol. 95, 41–60, 2022.

[23] Ali, W. A. E., A. A. Ibrahim, and A. E. Ahmed, "Dual-band millimeter wave 2 × 2 MIMO slot antenna with low mutual coupling for 5G networks," *Wireless Personal Communications*, Vol. 129, No. 4, 2959–2976, 2023.

[24] Sokunbi, O., H. Attia, A. Hamza, A. Shamim, Y. Yu, and A. A. Kishk, "New self-isolated wideband MIMO antenna system for 5G mm-Wave applications using slot characteristics," *IEEE Open Journal of Antennas and Propagation*, Vol. 4, 81–90, 2023.

[25] Alnemr, F., M. F. Ahmed, and A. A. Shaalan, "A compact 28/38 GHz MIMO circularly polarized antenna for 5G applications," *Journal of Infrared, Millimeter, and Terahertz Waves*, Vol. 42, No. 3, 338–355, 2021.

[26] El Halaoui, M., L. Canale, A. Asselman, and G. Zissis, "Dual-band 28/38 GHz inverted-F array antenna for fifth generation mobile applications," *Proceedings*, Vol. 63, No. 1, 53, 2020.

[27] Tadesse, A. D., O. P. Acharya, and S. Sahu, "A compact planar four-port MIMO antenna for 28/38 GHz millimeter-wave 5G applications," *Advanced Electromagnetics*, Vol. 11, No. 3, 16–25, 2022.

[28] Elsharkawy, R. R., K. F. A. Hussein, and A. E. Farahat, "Dual-band (28/38 GHz) compact MIMO antenna system for millimeter-wave applications," *Journal of Infrared, Millimeter, and Terahertz Waves*, Vol. 44, No. 11, 1016–1037, 2023.

[29] Hasan, M. N., S. Bashir, and S. Chu, "Dual band omnidirectional millimeter wave antenna for 5G communications," *Journal of Electromagnetic Waves and Applications*, Vol. 33, No. 12, 1581–1590, 2019.

[30] Tiwari, R. N., K. G. Malya, G. Nandini, P. B. Nikhitha, D. Sharma, P. Singh, and P. Kumar, "Quad-band 1 × 4 linear MIMO antenna for millimeter-wave, wearable and biomedical telemetry applications," *Sensors*, Vol. 24, No. 14, 4427, 2024.

[31] Sharma, M., B. R. Perli, L. Matta, T. Addepalli, K. Sharma, and F. N. Sibai, "Flexible four-port MIMO antenna for 5G NR-FR2 tri-band mmWave application with SAR analysis," *Scientific Reports*, Vol. 14, No. 1, 29100, 2024.

[32] Munir, M. E., M. M. Nasralla, and M. A. Esmail, "Four port tri-circular ring MIMO antenna with wide-band characteristics for future 5G and mmWave applications," *Heliyon*, Vol. 10, No. 8, e28714, 2024.